Severin Meyer

Strategy Optimization for the Bridgestone World Solar Challenge Using Dynamic Programming

Semester Project

Institute for Dynamic Systems and Control
Swiss Federal Institute of Technology Zurich
aCentauri Solar Racing

Supervision

Giona Fieni
Marc-Philippe Neumann
Prof. Dr. Christopher Onder

June 2023

IDSC-CO-GF-03

IDSC

aCE SOLAR RACING

Abstract

During the bi-annual *Bridgestone World Solar Challenge* over 40 teams from all over the world take on the difficult task of racing through the rough environment of the Australian Outback with their solar-powered cars on their 3000 km journey from Darwin to Adelaide via the famous Stuart Highway. This undertaking requires well-designed vehicles, which are able to master the significant technical challenges faced and a thought-through and robust race strategy in order to minimize the time needed to reach the destination. This Semester Project aims to optimize said race strategy and proposes a solution, which allows for rapid design iterations and changes in the road and environmental conditions, in order to give the *aCentauri Solar Racing Team* a versatile tool for this year's journey through Australia and all future races to come.

To find the ideal strategy and the global minimum for the total race time, a dynamic programming approach was chosen. Therefore, this report defines the optimal control problem which is the foundation of the optimization procedure, and describes its components in detail. This includes the used cost function, the system model, the initial and final conditions, and the acting constraints.

The report further describes the results originating from the optimization and presents the found strategy for the *Bridgestone World Solar Challenge*. Furthermore, the results for two different weather conditions are compared and the solar cars' performance is benchmarked with the data of other teams from previous competitions in order to set the expectations for the upcoming race.

Lastly, the report validates the optimization algorithm through correlation, by changing inputs and parameters and assessing the impact on the calculated strategy and whether the differences are in line with the expected behavior.

In the end, a working algorithm was created, and the goal of finding the optimal race strategy for the defined optimal control problem was achieved.

Keywords: Solar Racing, Strategy Optimization, Bridgestone World Solar Challenge, aCentauri Solar Racing, Dynamic Programming.

Acknowledgment

I would like to extend my deepest gratitude to the *Institute for Dynamic Systems and Control* at *ETH Zürich* and the *aCentauri Solar Racing Team* for hosting this Semester Project and for giving me the opportunity to work and learn in such a well-structured and inspiring environment. I would like to especially extend my sincere thanks to Giona Fieni and Marc-Philippe Neumann for supervising my work over the course of this venture and for contributing immensely to its success through their advice and guidance.

I'm extremely grateful to Dr. Stijn van Dooren for clearing up the many questions I had on the dynamic programming side of this project and for giving me the opportunity to deepen my understanding of the relevant theory of this topic.

Finally, my sincere thanks go to Giacomo Mastroddi for laying the foundation for my work with his Bachelor Thesis and for setting up the organizational structure for this Semester Project.

Contents

Nomenclature

Mathematical Symbols

α	Road Inclination	deg
$\Delta\vartheta$	Sandia Modeling Coefficient	-
η	Efficiency	-
κ	Sandia Modeling Coefficient	-
λ	Power Loss Coefficient	-
ν	Sandia Modeling Coefficient	-
ρ	Density	kg/m^3
Θ	MOI	$kg\,m^2$
ϑ	Temperature	$^\circ C$
A	Area	m^2
C	Friction Coefficient	-
E	Energy	J
e	Efficiency	-
F	Function	-
G	Horizontal Irradiance	W/m^2
g	Gravitational Constant	m/s^2
J	Cost Function	-
m	Mass	kg
N	Number of ...	-
P	Power	W
R	Real Coordinate Space	-
r	Radius	m
S	Insolation Level	mW/cm^2
SoC	State of Charge	%
T	Torque	N m
t	Time	s

U	Input Space	-
u	Input	W
v	Velocity	m/s
X	State Space	-
x	Distance	m

Subscripts

aero	Aerodynamic
amb	Ambient
bat	Battery
bear	Bear Ring
CF	Correction Factor
d	Drag
driv	Driver
dt	Drive Train
eff	Effective
el	Electric
f	Final
front	Frontal
grade	Gradiant
max	Maximal
mech	Mechanical
min	Minimal
mot	Motor
roll	Rolling
STC	Standard Condition
tot	Total
veh	Vehicle
w	Wheel

Acronyms and Abbreviations

BWSC	Bridgestone World Solar Challenge
CFD	Computational Fluid Dynamics
CS	Control Stop
DP	Dynamic Programming

ETH	Eidgenössische Technische Hochschule
IDSC	Institute for Dynamic Systems and Control
MOI	Moment of Inertia
MPC	Model Predictive Control
MPPT	Maximum Power Point Tracking
NOCT	Nominal Operating Cell Temperature
NS	Night Stop
OCP	Optimal Control Problem
PV	photovoltaic
SoC	State of Charge

Chapter 1

Introduction

This chapter will provide the background and foundation for the matters discussed in this report and places the technical discussion into context with the real-world application. Furthermore, the motivation behind the conducted research and its objectives are presented and an overview of the current state of research is given. Lastly, the structure of the report is introduced, to provide a better understanding of its flow of contents.

1.1 Context

1.1.1 aCentauri Solar Racing

Every year, teams consisting of third-year bachelor students from the *Department of Mechanical and Process Engineering* and the *Department of Information Technology and Electrical Engineering* of *ETH Zürich*, get the opportunity to take part in a "Focus Project" as part of their studies [1]. Here, they are able to tackle a challenging engineering task and develop a working prototype. Through this process, the students are able to put their theoretical knowledge into practice and grow as future engineers.

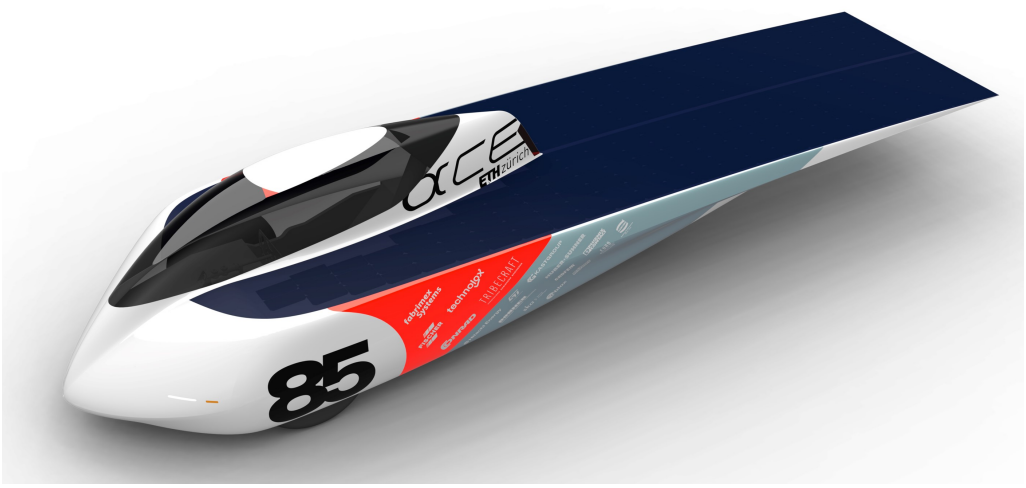

Figure 1.1: The *aCentauri Solar Racing* car design of 2023 [2] [3]

In September 2022 a team started working on building a solar-powered car in order to compete in the "Challenger Class" category of the BWSC and soon thereafter the *aCentauri Solar Racing* asso-

ciation was founded. As of the writing of this report, close to 50 students are actively contributing to the success of the ongoing project, distributed between the Focus Students from *ETH Zürich* and freelancers [3]. The team is structured into six sub-teams, each tackling a different aspect of the solar race car and the challenges faced in Australia. This project is conducted as part of the "Strategy and Simulation" sub-team, but in close cooperation with the other technical teams, due to multiple interfacing responsibilities.
The design envisioned for the race taking place in 2023 can be seen in figure 1.1.

1.1.2 Bridgestone World Solar Challenge

During the bi-annual *Bridgestone World Solar Challenge* over 40 teams from all over the world take on the difficult task of racing through the rough environment of the Australian Outback with their solar-powered cars on their 3000 km journey from Darwin to Adelaide via the famous Stuart Highway. Before the start of the race, all teams and solar cars must pass the so-called "scrutineering" by the race officials, in order to guarantee the readiness and safety of the vehicles [4] [5].

During the journey south, 9 "Control Stops" (CS) need to be passed, where the car needs to stand still for 30 minutes, while an inspection of the hardware takes place. During these stops, the solar car can still charge its battery with the energy coming from the sun. Furthermore, driving is only allowed between 8 am and 5 pm, such that sunlight is always available for the solar-powered cars and their drivers. Outside of these times, a "Night Stop" (NS) takes place, during which the car is not allowed to be driven or moved. Depending on how fast a team progresses down the route, between four and six NSs need to be conducted [5]. An overview of the route can be found in figure 1.2.

Figure 1.2: Route from Darwin to Adelaide [4]

The objective of the race is to reach the city of Adelaide as quickly as possible while complying with all of the guidelines of the competition.

1.2 Motivation

The engineers at the *aCentauri Solar Racing Team* have invested countless weeks, months and in some cases even more than a year of their free time into designing and testing this year's solar-powered race car. The motivation behind this Semester Project is to provide the team with an optimized race strategy, which allows for the best use of the build hardware, in order to place as high as possible on the leader-board of the *Bridgestone World Solar Challenge 2023*.

1.3 Objective

The primary objective of this semester project is to use a dynamic programming approach to define the ideal race strategy for the *Bridgestone World Solar Challenge* in order to find the global minimum for the final race time. To achieve this, all relevant system behaviors need to be modeled and the constraints of the race well defined. The final optimization result should reflect the real-world conditions as closely as possible.

1.4 State of Research

The relevant research areas for this Semester Project can be split into two areas: Modeling of solar-powered cars and dynamic programming optimization. In both cases, a large knowledge base to be used exists and the challenge of this project originates from the adaptation of these two disciplines to the regulatory framework of the *Bridgestone World Solar Challenge* and the exact solar race car design of the *aCentauri Solar Racing Team*.

- There are many sources available that document not only the modeling of standard vehicle dynamics but also specifically solar-powered cars [6] [7].
- The dynamic programming optimization approach is a well-known and widely used optimization method, with a wide knowledge base available to be leveraged at the *Institute for Dynamic Systems and Control* at *ETH Zürich* [8] [9] [10].

1.5 Outline

Chapter 1 outlines the background and foundation of the project and provides a description of the context, motivation, objectives, and the relevant state of research.

Chapter 2 focuses on the modeling of the solar-powered car and contains all formulas used to describe the state and input dynamics as well as the PV system and the electric motor. Furthermore, the meteorological conditions and the influences of the route are discussed.

Chapter 3 describes the standard definition of the optimal control problem. In addition to the system model, it contains the cost function, initial and final conditions, and constraints.

Chapter 4 contains the main results of the report. Here, the computed strategy for the whole race during the BWSC is presented. Additionally, a single race day and different weather scenarios are investigated and competition bench-marking is conducted.

Chapter 5 aims to show the validation through the correlation of the created optimization algorithm. Three different case studies are presented to highlight the functionality.

Chapter 6 ends the report by giving a conclusion of the work conducted during this Semester Project and identifies future work packages to improve the found strategy by presenting an outlook with possible next steps.

Chapter 2

System Modeling

The objective of this chapter is to define a mathematical model for all relevant dynamics of the solar race car, in order to describe its behavior correctly. Furthermore, the meteorological conditions and the characteristics of the route, which impact the driving performance, are introduced. To make the models in this chapter more understandable, they are formulated in the time domain, but the actual optimization is coded in the space domain. The switch between the two can simply be achieved with the translation equation seen in equation 2.1 [11].

$$\frac{dt}{dx} = \frac{1}{v} \tag{2.1}$$

2.1 Overview

The dynamic programming approach has the critical advantage, that not just a local, but the actual global minimum of an optimization problem can be found. This comes at a cost in the form of the computational requirements needed to solve for the ideal input profile. Due to this reason, the used models and necessary calculations should be held as simple as possible [8] [11].

In order to stick to simplicity, only four different systems are defined to describe the behavior of the solar race car: The battery, the photovoltaic system, the electric motor, and the vehicle dynamics. Another characteristic able to increase the computational requirements drastically is the number of states and inputs necessary to describe the system. Three states are defined: the State of Charge of the battery SoC, the velocity of the race car v, and its position x on the route from Darwin to Adelaide. As the input, the power drawn by the electric motor $P_{\text{mot,el}}$ is chosen. An overview of the system, its states, and input can be seen in figure 2.1.

2.2 Vehicle Dynamics

The basic theory behind the modeling of the dynamics of the vehicle originates from Newton's second law, which describes the change in momentum when a force acts upon an object. When using the power balance version of this law, the behavior of the system can be described with the separated system of differential equations seen in equations 2.2 and 2.3 [6] [7].

$$\dot{x} = v \tag{2.2}$$

$$\dot{v} = \frac{1}{m_{\text{tot}} \cdot v} \cdot (P_{\text{mot,mech}} - P_{\text{aero}}(v, x, t) - P_{\text{grade}}(v, x) - P_{\text{roll}}(v, x) - P_{\text{bear}}(v)) \tag{2.3}$$

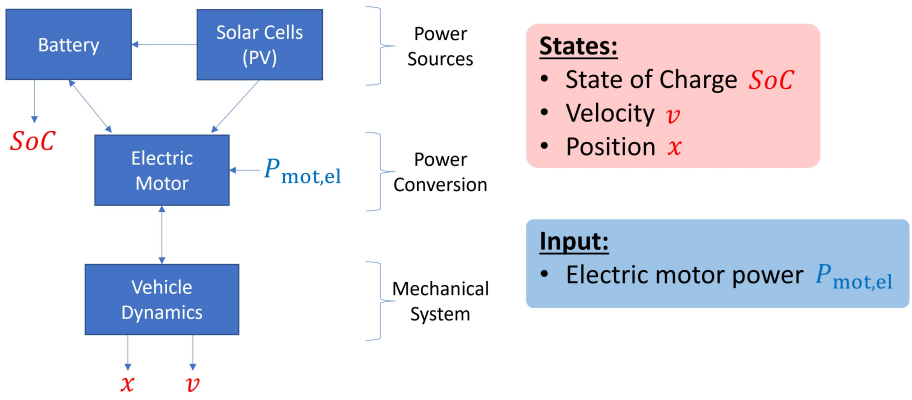

Figure 2.1: System modeling overview

Here, x describes the distance from the start of the race, and v is the current velocity of the solar race car. m_{tot} is the total mass of the system, $P_{\text{mot,mech}}$ the output of mechanical power from the electric motor, P_{aero} is the aerodynamic loss originating from the drag force, P_{roll} the power loss through the rolling friction of the wheels, P_{grade} the power loss through the current slope of the road, and P_{bear} the friction power losses in the bear rings. The detailed equations for these power losses can be found in equations 2.4 to 2.7.

$$P_{\text{aero}}(v,x,t) = \frac{1}{2} \cdot \rho(x) \cdot C_{\text{d}} \cdot A_{\text{front}} \cdot v_{\text{front,eff}}^2(v,x,t) \cdot v \tag{2.4}$$

$$P_{\text{grade}}(v,x) = m_{\text{tot}} \cdot g \cdot \sin(\alpha(x)) \cdot v \tag{2.5}$$

$$P_{\text{roll}}(v,x) = m_{\text{tot}} \cdot g \cdot C_{\text{roll}} \cdot \cos(\alpha(x)) \cdot v \tag{2.6}$$

$$P_{\text{bear}}(v) = \left(\frac{N_{\text{front}} \cdot T_{\text{front}}}{r_{\text{w}}} + \frac{N_{\text{rear}} \cdot T_{\text{rear}}}{r_{\text{w}}} \right) \cdot v \tag{2.7}$$

Where ρ is the density of the air, A_{front} the frontal aerodynamic cross-section, C_{d} the drag coefficient, C_{roll} the rolling friction coefficient, g the gravitational constant, α the road inclination, N_{front} the number of frontal bear rings, N_{rear} the number of rear bear rings, T_{front} the front bear ring friction torque, T_{rear} the rear bear ring friction torque and r_{w} the wheel radius. $v_{\text{front,eff}}$ is the effective frontal airspeed and can be calculated as seen in (2.8).

$$v_{\text{front,eff}}(v,x,t) = v + v_{\text{front,wind}}(x,t) \tag{2.8}$$

The total mass of the solar race car m_{tot} can be found by adding the mass of the driver m_{driv}, fixed to 80 kg by the competition [5], and the equivalent rotational mass of the drive train m_{dt} to the mass of the vehicle itself m_{veh}, as seen in equation 2.9.

$$m_{\text{tot}} = m_{\text{veh}} + m_{\text{driv}} + m_{\text{dt}} \tag{2.9}$$

The equivalent mass contribution of the drive train can be found with equation 2.10 [6].

$$m_{\text{dt}} = \frac{\Theta_{\text{front,dt}}}{r_{\text{w}}^2} \tag{2.10}$$

Where Θ_{dt} is the moment of inertia of all rotating parts and r_w is the wheel radius. This effect adds 14.6 kg to the total mass of the solar race car.
An overview of the constant parameters can be seen in table 2.1. Some parameters, such as the aerodynamic drag and the rolling friction coefficient, are assumed to be constant, even though they are a function dependent on the velocity of the car. The aerodynamic drag coefficient was estimated with CFD simulations with an airspeed of 85 $^{km}/_{h}$ [12].

Table 2.1: Vehicle dynamics parameter overview

Parameter	**Symbol**	**Value**
Average air density	ρ	1.17 $^{kg}/_{m^3}$
Drag coefficient	C_d	0.09
Frontal area	A_{front}	0.85 m^2
Gravitational constant	g	9.8067 $^{m}/_{s^2}$
Rolling friction coefficient	C_{roll}	0.003
Number of front bearings	N_{front}	4
Front bearing friction torque	T_{front}	0.055 N m
Number of rear bearings	N_{rear}	1
Rear bearing friction torque	T_{rear}	0.2 N m
Wheel radius	r_w	27.85 cm
Vehicle mass	m_{veh}	150 kg
Driver mass	m_{driv}	80 kg
MOI of drive train	Θ_{dt}	1.134 kg m^2

2.3 Electric Motor Model

The purpose of the electric motor is to convert the electrical power provided by the photovoltaic system and the battery into mechanical power, in order to control the vehicle dynamics. For the description of the behavior of the electric motor, the Williams model can be used and can be seen in equation 2.11 [6]. One has to note that the powered wheel is directly attached to the electric motor, leading to a transmission ratio of one, and therefore the modeling of the power train can be simplified. Furthermore, the model differentiates between the recuperation case, where the kinetic energy of the car is transferred into the battery, and the usual power transfer to the vehicle dynamics to propel the solar-powered car forward.

$$P_{mot,mec}(P_{mot,el}) = \begin{cases} P_{mot,el} \cdot e_{mot} - P_0 & , if P_{mot,el} \geqslant P_0 \\ \frac{P_{mot,el}}{e_{mot}} - P_0 & , if P_{mot,el} < P_0 \end{cases} \tag{2.11}$$

An overview of the electric motor constants can be seen in table 2.2. The electric motor efficiency can usually be described in the form of an electric motor efficiency map, but for the sake of simplicity and due to the lack of such testing data, the value is approximated to be constant [12].

Table 2.2: Electric motor model parameter overview

Parameter	**Symbol**	**Value**
Electric motor efficiency	e_{mot}	0.97
Idle loss	P_0	30 W

2.4 Battery Dynamics

The battery dynamics are described by the change in the State of Charge, which can be formulated as the difference between the power provided by the photovoltaic system and the power drawn by the electric motor. The formulation of this behavior can be seen in equation 2.12 [7] [6].

$$\dot{SoC} = \frac{P_{\mathrm{PV}}(v,x,t) - P_{\mathrm{mot,el}}}{E_{\mathrm{bat,max}}} \tag{2.12}$$

Where $E_{\mathrm{bat,max}}$ is the maximum energy capacity of the battery. In the current solar-powered car design this value is 5.2 kWh.

2.5 PV Model

The purpose of the photovoltaic system is to convert the solar radiation provided by the sun into electric power. The model can be formulated into equation 2.13 [13].

$$P_{\mathrm{PV}} = A_{\mathrm{PV}} \cdot G(x,t) \cdot \eta_{\mathrm{PV}} \cdot \eta_{\mathrm{CF}}(v,x,t) \cdot \eta_{\mathrm{loss}} \tag{2.13}$$

Where P_{PV} is the power output of the photovoltaic system, A_{PV} is the area of the solar panels, G is the total global irradiance, η_{PV} the general efficiency of the panels, η_{CF} is the correction factor for the temperature of the solar cells, and η_{loss} the conversion loss coefficient, which can be split into the wire, MPPT, and mismatch efficiencies as seen in equation 2.14 [14].

$$\eta_{\mathrm{loss}} = \eta_{\mathrm{wire}} \cdot \eta_{\mathrm{MPPT}} \cdot \eta_{\mathrm{mismatch}} \tag{2.14}$$

The η_{wire} efficiency accounts for the losses in the wires, η_{MPPT} models the losses due to the imprecision of the MPPT device, and η_{mismatch} models the losses originating from the off-set between the operation and maximum power point.

The temperature efficiency correction is modeled through equation 2.15 [13].

$$\eta_{\mathrm{CF}} = 1 - \lambda_{\mathrm{PV}} \cdot (\vartheta_{\mathrm{PV}}(v,x,t) - \vartheta_{\mathrm{STC}}) \tag{2.15}$$

Here, λ_{PV} is the power loss coefficient, ϑ_{STC} the standard condition temperature, and ϑ_{PV} the actual temperature of the solar cells. Due to the difficulty of the system identification process, the value for the temperature of the solar cells was set equal to the standard temperature. Two models are currently being investigated to represent the temperature of the PV system more accurately: The Sandia and NOCT model.

The Sandia model is a quite detailed approach since it not only takes the thermodynamic characteristics of the PV setup into account but also the wind blowing over the solar cells with its cooling effect. The Sandia model can be seen in equation 2.16 [13].

$$\vartheta_{\mathrm{PV}}(v,x,t) = G(x,t) \cdot \exp(\nu + \kappa \cdot v_{\mathrm{eff}}(v,x,t)) + \vartheta_{\mathrm{amb}}(x,t) + \frac{G(x,t)}{G_0} \cdot \Delta\vartheta \tag{2.16}$$

Here, ν, κ, and $\Delta\vartheta$ are coefficients to be experimentally determined and G_0 is the reference global irradiance of $1000\,\mathrm{W/m^2}$.

The effective speed of the airflow over the solar PV panels v_{eff} can be calculated with equation 2.17.

$$v_{\text{eff}}(v, x, t) = v + v_{\text{wind}}(x, t) \tag{2.17}$$

Where v is the current velocity state of the vehicle and v_{wind} the wind speed, depending on time and position. Note that this is a vector formula, since the directions of v and v_{wind} are generally not aligned.

The NOCT model is a much simpler approach and can be seen in equation 2.18 [15].

$$\vartheta_{\text{PV}}(x, t) = \vartheta_{\text{amb}}(x, t) + \frac{\vartheta_{\text{NOCT}} - 20}{80} \cdot S \tag{2.18}$$

Here only the value for the NOCT temperature ϑ_{NOCT} and the insulation level S need to be determined experimentally.

An overview of the constant parameters of the PV system can be found in table 2.3.

Table 2.3: PV model parameter overview

Parameter	**Symbol**	**Value**
Area of solar panels	A_{PV}	$4\,\text{m}^2$
PV efficiency	η_{PV}	0.244
Wiring efficiency	η_{wire}	0.98
MPPT efficiency	η_{MPPT}	0.99
Mismatch efficiency	η_{mismatch}	0.98
Power loss coefficient	λ_{PC}	$0.0029\,{}^{1}/_{^\circ\text{C}}$
Standard-conditioning temperature	ϑ_{STC}	$25\,^\circ\text{C}$
Reference global irradiance	G_0	$1000\,{}^{\text{W}}/_{\text{m}^2}$

2.6 Meteorological Conditions

Due to the technical nature of the system and the setting of the competition, the weather has a decisive influence on the performance of the solar race car. The relevant variables are the following: the global irradiance, the frontal wind speed acting against or with the car's direction of movement, and the ambient temperature. All of these variables are generally functions of space and time, but for simplicity and due to a lack of data, only time-dependent global irradiance is used for the optimization.

2.6.1 Global Irradiance

The total global irradiance describes how much power the sun projects onto each square meter of a flat surface. Measured high-resolution data from the year 2020 with time steps of only one minute is used for the optimization presented in this report [16]. The values originate from the town of Alice Springs around the midpoint of the Stuart Highway. The advantage of this is that real-world data can be used, but ideally, mean values averaged over multiple years would have been better for the purpose of this project. Figure 2.2 shows the global irradiance on the dates of the competition during the active race time between 8 am and 5 pm. The fourth day shown in figure 2.2, represents the ideal weather conditions, due to an almost perfect global irradiance profile over the entire race day. The significant drops seen during the first, third, and fifth race days originate from a high level of cloud cover.

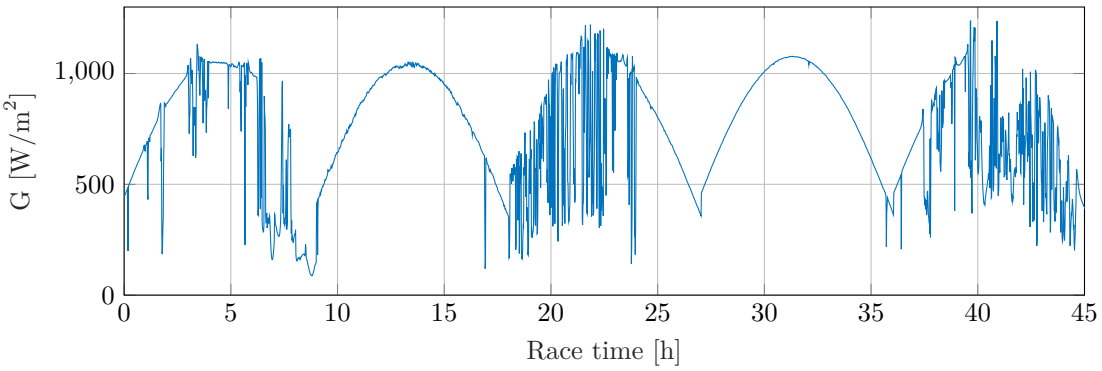

Figure 2.2: Global irradiance in time domain (Alice Springs)

2.6.2 Frontal Wind

Since the route to be driven is already known in advance of the competition, the direction the car will be facing at a specific location is known. With this knowledge, the frontal wind speed acting against or with the car's direction of movement, which is needed for the drag calculations, can be determined. Figure 2.3 shows the time and space dependency of this variable. The wind and temperature data used are averaged values of the past 50 years, with a time and spatial resolution of 1 h and 5 km respectively, provided by the *Institute for Atmospheric and Climate Science* at *ETH Zürich* [17].

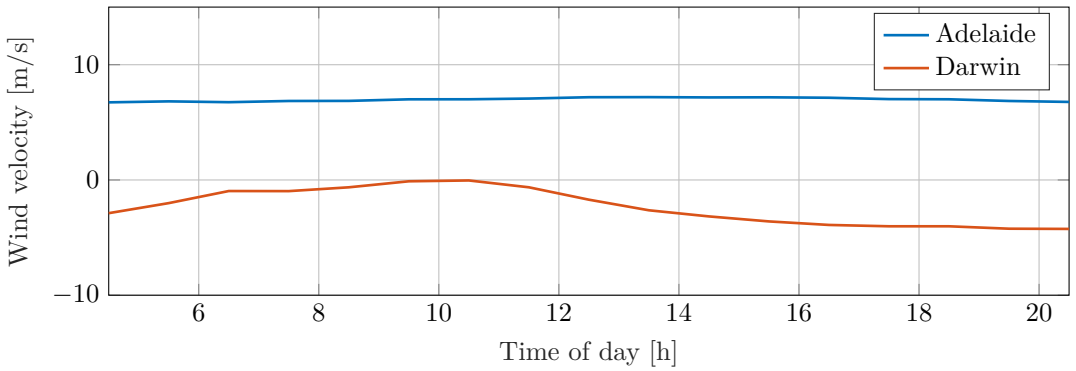

Figure 2.3: Frontal wind in time domain

The meteorological behavior of wind generally blowing from the high-density cold zones over the ocean to the low-density hot zones over the land area can be seen, since the solar car gets a boost driving away from the water in Darwin in the north and having to fight its way towards the ocean in the south near Adelaide.

2.6.3 Ambient Temperature

Similar to the wind data, the time and space dependency of the ambient temperature can be seen in Figure 2.4 [17].

Here the meteorological behavior also corresponds with the expectations. Darwin in the North and therefore closer to the equator shows a significantly higher ambient temperature during the time window of the competition than Adelaide in the South.

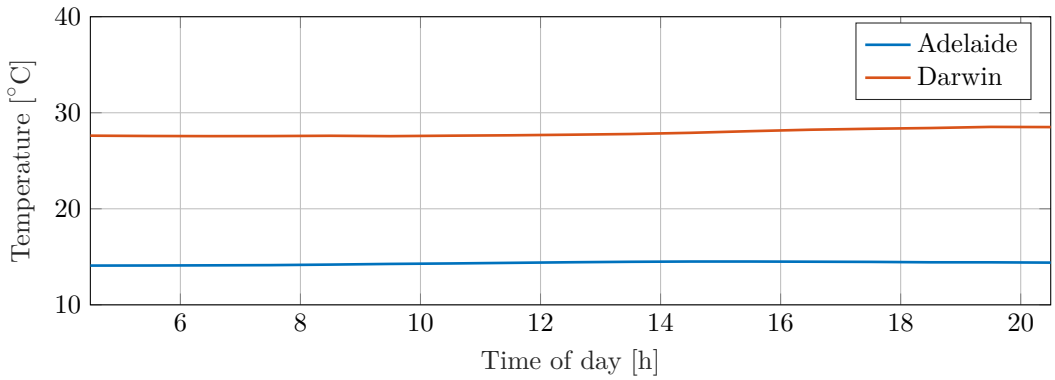

Figure 2.4: Temperature in time domain

2.7 Route on Stuart Highway

The characteristics of the route have a large influence on the driving behavior of the solar-powered car and are therefore of high significance to the race optimization. The following two variables are considered in the calculations: the altitude of the route and the current inclination. The data used during this project originates from the *Brouter* web page [18].

2.7.1 Elevation

The altitude profile over the 3000 km distance of the race can be seen in Figure 2.5.

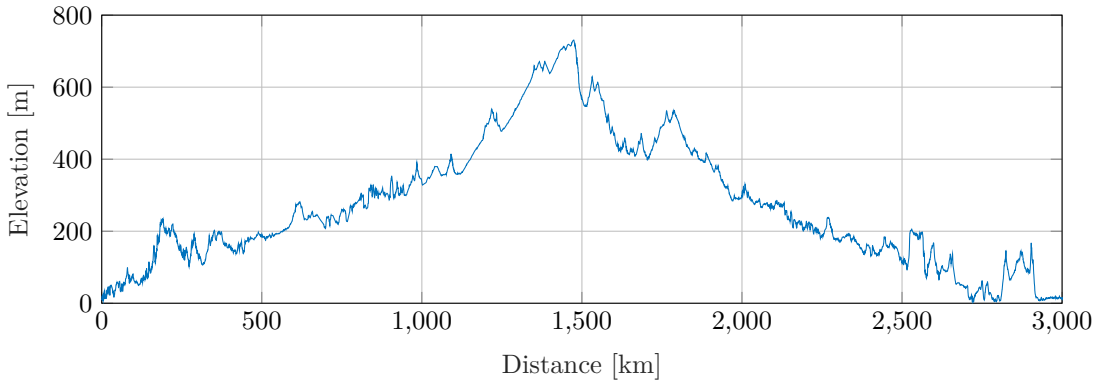

Figure 2.5: Elevation in space domain

It can be noted that during the first part of the race, the altitude tends to increase, whereas a general decrease can be seen during the second half. Both the start and the end of the race are at sea level and the maximum altitude reached is around 700 m. This value has two significant effects on the optimization: The dynamic programming algorithm needs to know that during the first half of the race potential energy will be stored, due to the general increase in elevation, which will be released during the second half of the race. Furthermore, the altitude has an impact on the density of the air, which affects the drag force experienced by the car.

2.7.2 Inclination

The inclination of the road is the derivative of the altitude and is needed for the power losses due to the road's elevation and the rolling friction, as can be seen in equations 2.5 and 2.6. The inclination profile of the road can be seen in Figure 2.6.

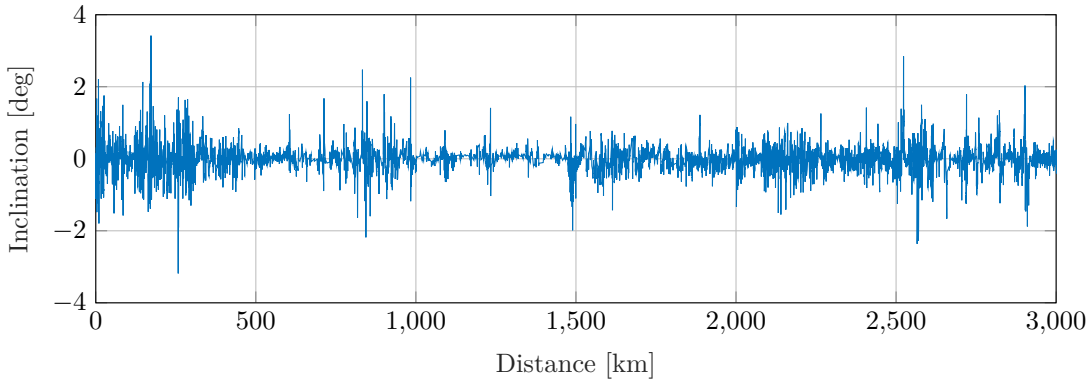

Figure 2.6: Inclination of the road in the space domain

Chapter 3

Optimal Control Problem

The purpose of this chapter is to define the optimal control problem for race optimization. Here the general structure from academia is used, where the following components need to be determined, in order to define the OCP fully: The cost function, the system model, the initial and final conditions, and the state and input constraints, as seen in equation 3.1 [8] [9]. The system model is already discussed in chapter 2.

$$\text{OCP} = \begin{cases} \min_{u(t)} J(u(t)) & \rightarrow \text{ Cost Function} \\ s.t. & \\ \dot{x}(t) = F(x(t), u(t), t) & \rightarrow \text{ System Model} \\ x(0) = x_0 & \rightarrow \text{ Initial Conditions} \\ x(t_\text{f}) \in [x_{\text{f,min}}, x_{\text{f,max}}] & \rightarrow \text{ Final Conditions} \\ x(t) \in X(t) \subset R^n & \rightarrow \text{ State Constraints} \\ u(t) \in U(t) \subset R^m & \rightarrow \text{ Input Constraints} \end{cases} \tag{3.1}$$

3.1 Cost Function

The cost function can be efficiently defined by looking at the goal of the BWSC competition: Finish the race from Darwin to Adelaide as fast as possible [5]. Therefore, the variable to minimize is the total race time. The final cost function in the time and space domain can be seen in equation 3.2.

$$\min_{P_\text{mot,el}} J(P_\text{mot,el}) = \min_{P_\text{mot,el}} \int_0^t dt = \min_{P_\text{mot,el}} \int_0^x \frac{1}{v} dx \tag{3.2}$$

3.2 Initial and Final Conditions

In order to properly define our OCP, the initial and final conditions for our states, SoC, velocity, and position, as well as the race time need to be defined. The chosen initial condition can be seen in equations 3.3 to 3.6.

$$SoC_0 = 100\,\% \tag{3.3}$$

$$v_0 = 65\,\text{km/h} \tag{3.4}$$

$$t_0 = 0\,\mathrm{s} \tag{3.5}$$

$$x_0 = 0\,\mathrm{km} \tag{3.6}$$

The race is initiated with the maximal charge available in the battery, at a velocity of $65\,\mathrm{km/h}$, a distance of 0 km, and a time of 0 s. The initial condition for the velocity is chosen, such that it compiles with the speed constraints at the beginning of the route as described in section 3.3.1. Over a race distance of 3000 km, this value has a negligible effect.

As a final condition, as seen in equation 3.7, only the traveled distance is set to the finish line at 3000 km. All other state variables are able to free float, such that the DP is able to work with the largest solution space possible.

$$x_\mathrm{f} = 3000\,\mathrm{km} \tag{3.7}$$

3.3 Constraints

The really challenging and critical part of this OCP is the definition and implementation of the constraints. There are two sources for the constraints acting upon the system: The technical limitations of the solar-powered race car and the rules defined by the competition. These can be split up into three sections: constraints acting on states, including the time variable, the input, and the control and night stops imposed by the competition.

3.3.1 State Constraints

In total, three state constraints need to be defined. The competition imposes the regulation that the speed limit of the public roads needs to be respected, which creates an upper bound for the velocity state [5]. Furthermore, the high-speed sections of the Stuart highway actually have a minimum speed requirement of $60\,\mathrm{km/h}$ which the car needs to surpass. Since the Steward highway also passes through towns and small cities with lower speed limits, this constraint is space-dependent, as can be seen in equation 3.8.

$$v_\mathrm{min}(x) \leqslant v \leqslant v_\mathrm{street}(x) \tag{3.8}$$

The upper-speed limit over the entire route can be seen in figure 3.1. Please note that for the simulations a discretization of between 5 km and 10 km in the space domain is used, where the speed limit in these sections is averaged. Therefore the speed limit boundaries are different in the optimization results presented in chapter 4 and 5.

The next constraint originates from the technical and physical limitations of the batter. The *SoC* cannot surpass the 100 % mark. Furthermore, the *aCentari Solar Racing Team* decided, that a 10 % *SoC* reserve shall be present at all stages of the race [12]. The complete *SoC* constraint can be seen in equation 3.9.

$$SoC \geqslant 10\,\% \tag{3.9}$$

Lastly, the active driving time needs to be between 8 am and 5 pm. There is some slack in the regulations: When stopping up to 10 min after 5 pm, the additional time will be added the next morning without penalty. So if the team would stop at 5:07 pm, it will be allowed to continue at 8:07 am the next day [5]. The constraint can be seen in equation 3.10.

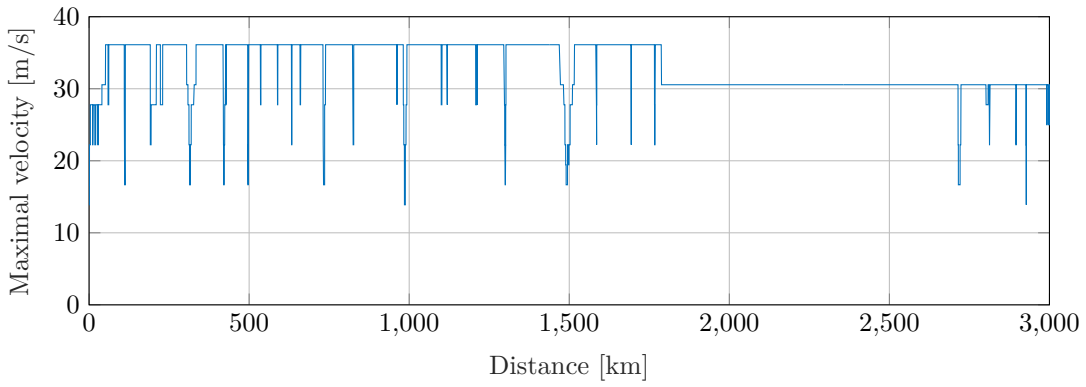

Figure 3.1: Maximal velocity allowed on route from Darwin to Adelaide

$$8{:}00 \leqslant t \leqslant 17{:}00 \tag{3.10}$$

3.3.2 Input Constraints

There is only a single input constraint acting upon the solar race car and it originated from the technical limitation of the electric motor: It can only recuperate and transmit power in the range of $-5\,\mathrm{kW}$ and $5\,\mathrm{kW}$, as seen in equation 3.11.

$$-5\,\mathrm{kW} \leqslant P_{\mathrm{mot,el}} \leqslant 5\,\mathrm{kW} \tag{3.11}$$

3.3.3 Stop Constraints

There are two stop constraints originating from the regulations of the competition: Control Stop and Night Stop conditions [5].

Control stops are space-dependent pre-defined constraints, which means that the starting time of these stops is not known in advance. There are 9 planned checkpoints distributed on the route from Darwin to Adelaide. At these control stops the car is expected to stand still for 30 min and to be inspected by the race officials to guarantee the safety of the car. During this time the car is still allowed to charge by using its photovoltaic system. The control stop condition can be seen in equation 3.12.

$$if\ x = [Stop1, Stop2, ...] \quad \rightarrow \quad Control\ Stop\ (CS)\ Condition \tag{3.12}$$

In order to not run out of energy, the solar-powered cars of the competition need a constant supply of solar energy. Due to this reason, the officials from the competition have decided to only allow active driving between 8 am and 5 pm each race day. This is a time-dependent constraint, which means that it won't be known in advance, where exactly in the space domain the car needs to stop during the race. This is subject to the optimization of the race strategy. The night stop condition can be seen in equation 3.13.

$$if\ t = 17{:}00 \quad \rightarrow \quad Night\ Stop\ (NS)\ Condition \tag{3.13}$$

One has to consider the scenario where a Control Stop takes after 4:30 pm. Here, the additional CS time which goes past 5 pm, will be added to the starting time the next day. For example, when the car gets to a CS location at 4:47 pm, the team will be allowed to continue at 8:17 am the next day.

Chapter 4

Race Optimization Results

This chapter presents the main result of this Semester Project: It discusses the optimized strategy for the full race and the first race day, as well as compares the full race optimization with a scenario using different weather data. Furthermore, it sets the results into comparison with the performance of other competing teams in the form of competition bench-marking. The dynamic programming optimization is based on proprietary algorithms developed by the *IDSC* at *ETH Zürich* [10].

4.1 Optimization of Whole Race

The results for the optimization in the form of the SoC, velocity, and input profiles over the entire distance of 3000 km can be seen in figures 4.1, 4.2, and 4.3 respectively. The resolution in the space domain was chosen to be 10 km due to computational considerations.

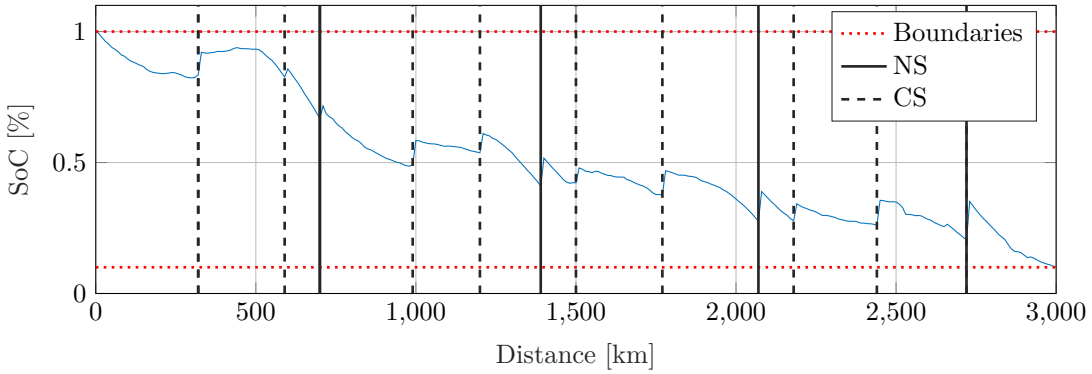

Figure 4.1: Optimization results for whole race (SoC in space domain)

The SoC profile in figure 4.1 clearly shows the influence of the control and night stops, which are marked by dashed and solid lines respectively.
Each time the car stops it is able to charge the battery partially with the PV system, which leads to a step-like increase in the SoC graph. Furthermore, one can observe that the SoC tends to decrease faster at the beginning and the end of each race day, due to the low global irradiance available as an energy source. During the mid-day hours, the energy profile can mostly be kept at quite a steady level and the system is able to drive in a power-neutral way from the point of view of the battery. It can also be noted that the optimization guides the SoC exactly to 10 % at the end of the race. This is a very intuitive decision made since the system's objective is to reach the destination as fast as possible and therefore uses the maximal amount of energy available to it.

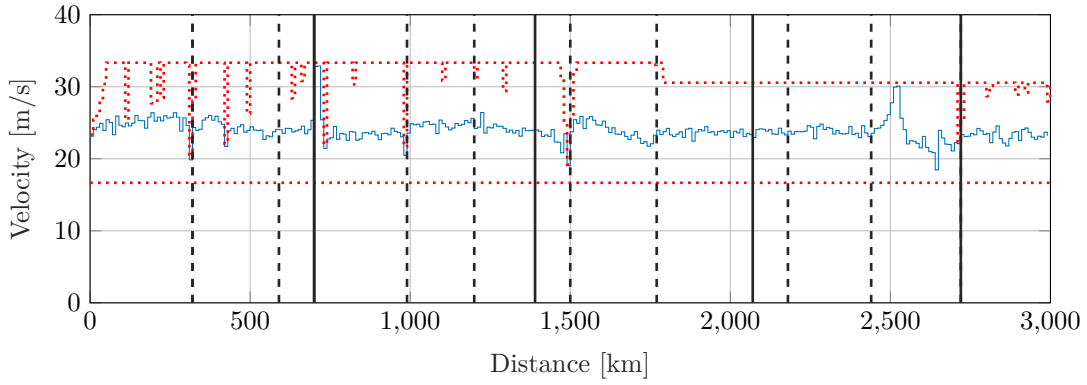

Figure 4.2: Optimization results for whole race (Velocity in space domain)

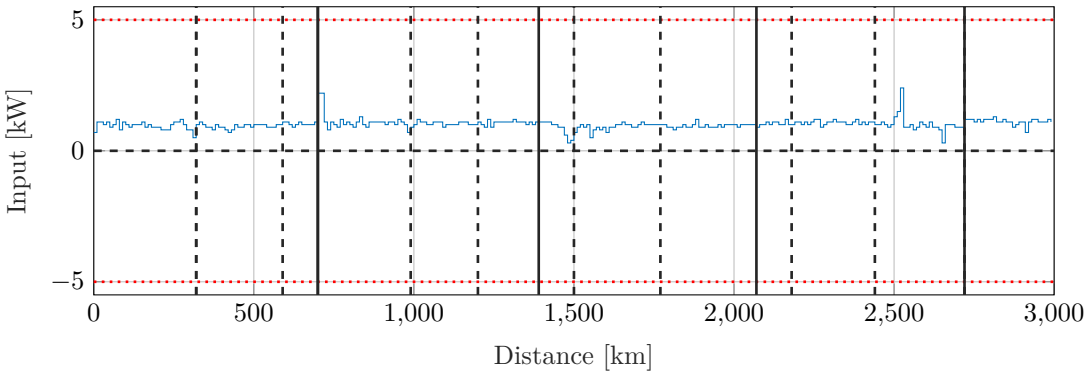

Figure 4.3: Optimization results for whole race (Input in space domain)

When inspecting the velocity and input profiles in figures 4.2 and 4.3 more closely, the clear physical relationship between the two values can be seen: An increase in input power to the electric motor leads to higher velocities of the solar-powered car.
Furthermore, both profiles are in general quite steady, and only a few deviations from the average value can be seen. This is in line with the real-world use case: The BWCS is a long-range endurance race and the proposed models do not incorporate drastic maneuvers, such as overtaking or driving very tight corners. It can also be seen that the boundaries originating from the state and input constraints, described in section 3.3, are never violated.

The optimized input profile guides the car over the finish line within an active driving time of 39 h and 26 min with an average velocity of 86.1 $^{\mathrm{km}}/_{\mathrm{h}}$. The computational time for the shown results was 9 h and 30 min.

4.2 Optimization of First Race Day

Due to the computational requirements of the dynamic programming optimization, the discretizations of the space, state, and input domains were chosen to be quite coarse for the 3000 km of the entire race. Another optimization was now done with a higher resolution of 5 km for the first 800 km of the route. This represents 100 km more than what can be achieved on the first day. For the final condition, the *SoC* target was set equivalently to what the whole race results predicted at the 800 km mark.

Figures 4.4, 4.5, and 4.6 show the SoC, velocity and input profiles of this case. The same general observations, regarding the system behavior and optimization results, as described in section 4.1, can be made here as well.

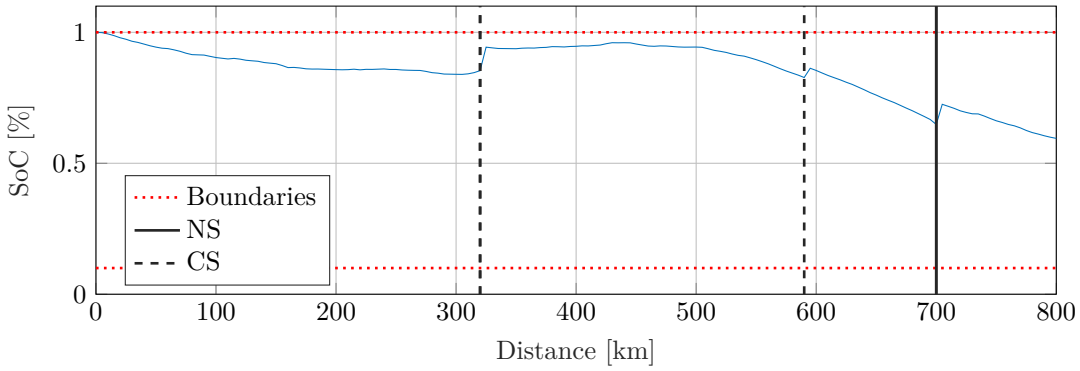

Figure 4.4: Optimization results of first race day (SoC in space domain)

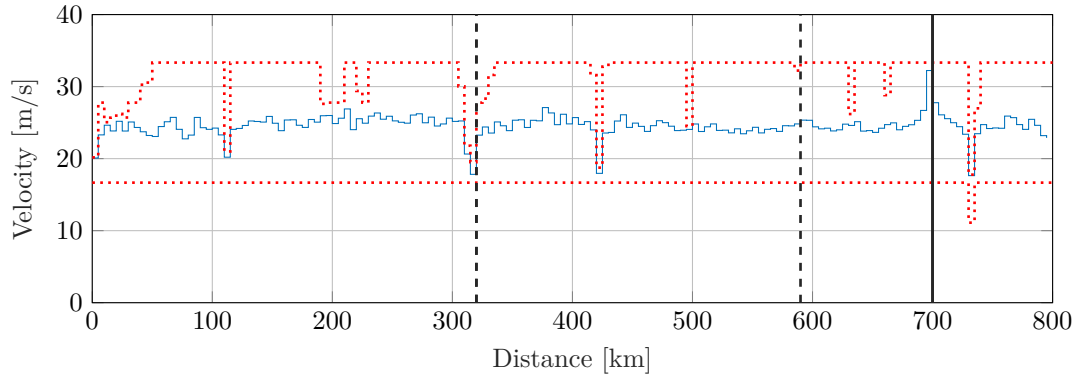

Figure 4.5: Optimization results of first race day (Velocity in space domain)

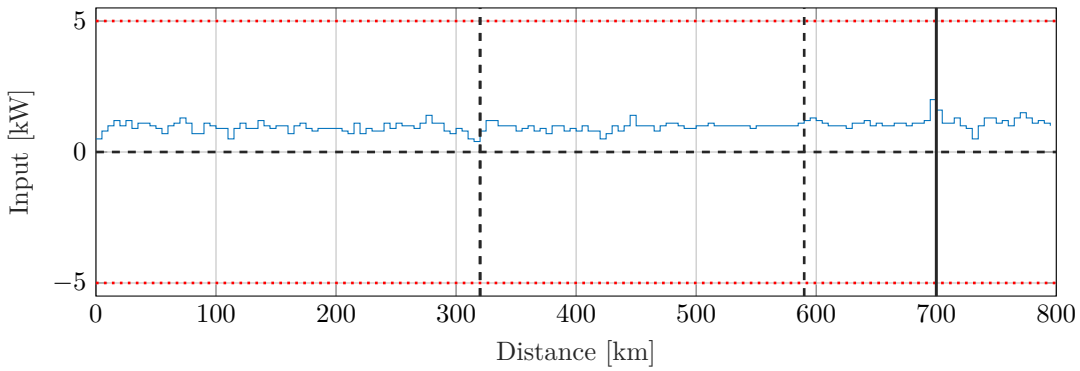

Figure 4.6: Optimization results of first race day (Input in space domain)

When comparing the SoC results presented in this chapter with the whole race optimization in the first 800 km, as shown in figure 4.7, some interesting observations can be made: Due to the discretization of the optimization, two different profiles were found. However, the significant value

of the time the solar-powered car needs to travel the defined distance is very close, with a difference of only 5 min. Noteworthy here is that the slower solution also ends the race with a higher final *SoC* value, which means the solutions are even closer when taking the total energy spent into account. This example shows, that there are countless solutions to the given problem, due to local minima found by the optimization, and the output heavily depends on the discretizations used.

The optimized input profile guides the car to 800 km within an active driving time of 10 h and 6 min with an average velocity of 88.2 $^{km}/_{h}$. The computational time for the shown results was 6 h and 11 min.

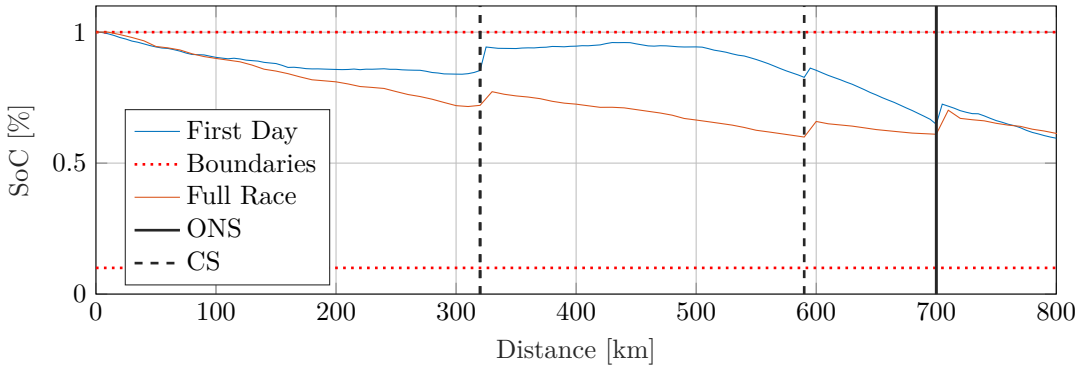

Figure 4.7: Comparison *SoC* profiles whole race and first race day optimization

4.3 Optimization with Improved Weather Conditions

When analyzing the weather data from October 2020, the days of the competition that year have a large amount of cloud cover, as discussed in section 2.6.1. When taking other days from the data set available from October 2020, a better time frame can be chosen. One of these options can be seen in figure 4.8.

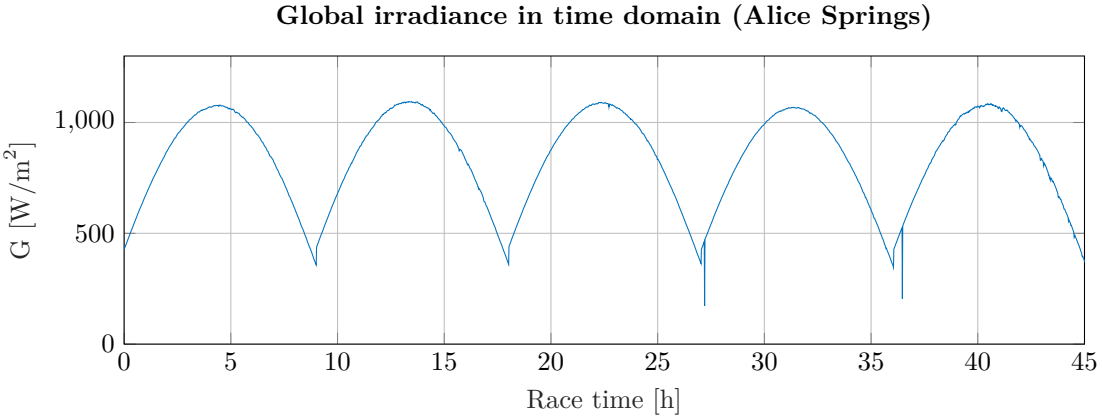

Figure 4.8: Ideal global irradiance profile taken from October 2020 weather data

When optimizing the race under these improved weather conditions a better race performance is to be expected. The comparison between the two *SoC* profiles from the results discussed in section 4.1 and the current case can be seen in figure 4.9.

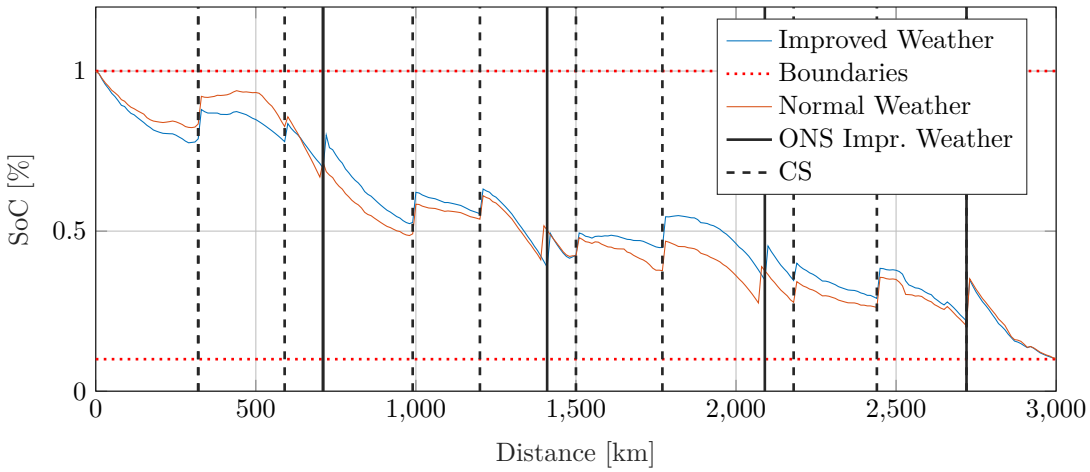

Figure 4.9: Comparison between SoC profile of standard and improved weather conditions

The results show that the improved weather case has more energy available over the course of the race. On average, an increase in global irradiance of 92 $^{W}/_{m^2}$ is provided to the PV system under ideal weather conditions.
Figure 4.9 shows the SoC of the improved weather case being generally higher. One can also note that the majority of night stops are reached with more distance covered in the case of more global irradiance available. In the end, the better weather conditions only lead to a very minor reduction in the final race time of 4 min.

The optimized input profile of the improved weather case guides the car to the finish line within an active driving time of 39 h and 22 min with an average velocity of 86.2 $^{km}/_{h}$. The computational time for the shown results was 9 h and 30 min.

4.4 Competition Bench-marking

The race results for the past BWSC competitions are openly available. In figure 4.10 the data from the years 2019 and 2017 is shown. From the optimization presented in section 4.1 we know the expected average velocity of the solar-powered car and the results can be added to the graph in figure 4.10 to compare the optimized performance to the other competing teams. As a caveat, it needs to be mentioned, that the global irradiance data from the year 2020 was taken for the optimization, which differs from the conditions which were present in the years 2019 and 2017.

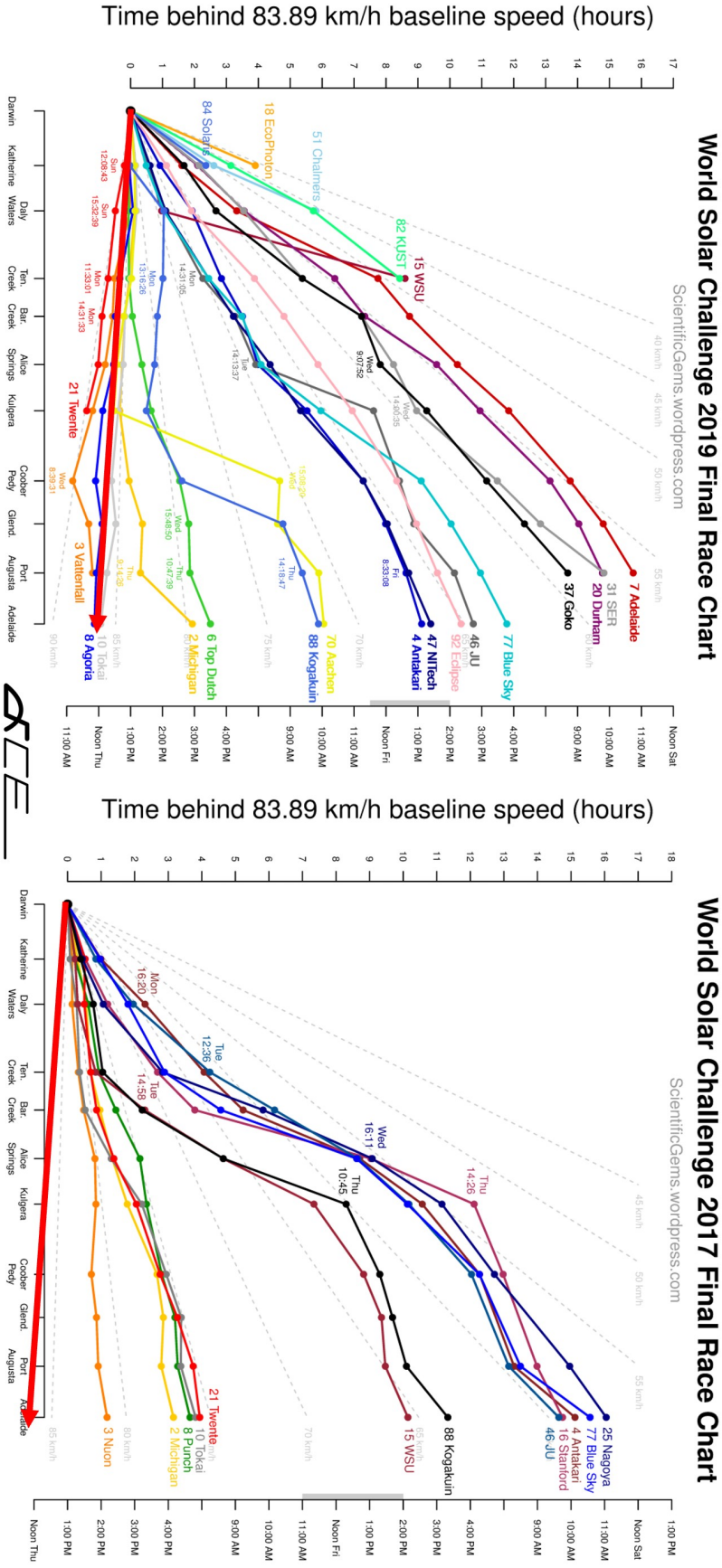

Figure 4.10: Race optimization results compared with competition results from 2019 and 2017

Chapter 5

Case Studies

This chapter presents the results of the conducted case studies. The objective is to show the functionality of the optimization algorithm. To achieve this, different parameters and inputs, such as the weather data, of the models are varied and the effects on the results are recorded. In case the trend shown correlates with the expected behavior of the system, the optimization results can be categorized as being sound estimations of the solar-powered car's characteristics.
Therefore, four values are defined in order to break the results into a meaningful and easy-to-present format: the final race time, the final SoC, the average velocity, and the average input. When, for example, the total energy available to the system is increased, it can be expected for the final race time to be lower and the average velocity and input to be higher, as long as the solar-powered car is energy constrained. If not, the final SoC will increase while the other values stay the same.
Three different case studies are presented in this chapter: a battery sweep, a solar parameter sweep, and a solar wall sweep.

5.1 Case Study 1: Battery Sweep

A battery sweep is a common case study for optimization algorithms with battery-powered vehicles or devices. The objective is to run the system through the same optimization scenario with a varying target value for the final SoC. If this value is set higher, the total energy available to the system is lower and a corresponding behavior is expected.
The battery sweep in this report optimizes the first 800 km of the race and varies the final SoC between 20 % and 90 % with steps of 10 %. The optimization for each iteration took a computational time of 10 min.

5.1.1 Results

The results for the cases targeting a final SoC between 20 % and 80 % can be seen in figure 5.1.

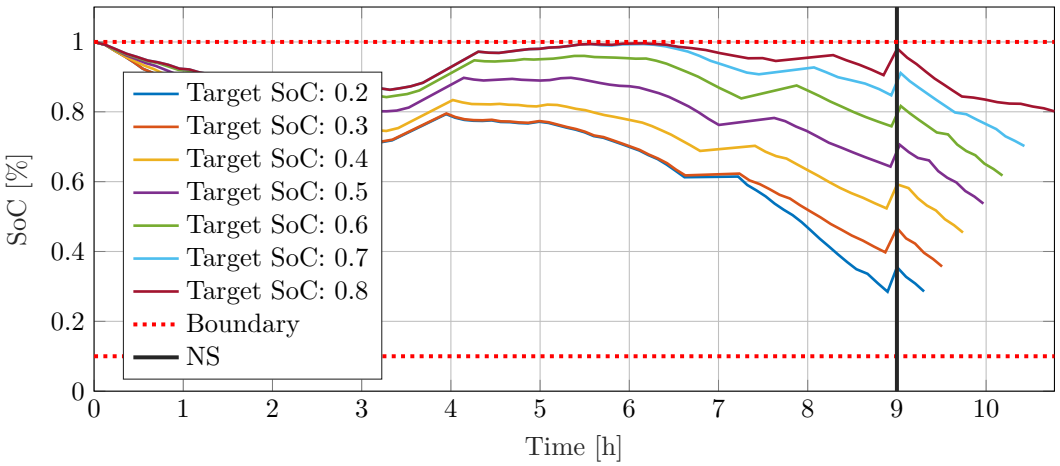

Figure 5.1: Battery sweep in time domain (target SoC between 20 % and 80 %)

The SoC profiles track their target $SoCs$ in similarly shaped patterns. Furthermore, it can be noted that, since the system is energy constrained in this case, the final time of the race becomes larger if the targeted SoC is higher. This can be seen clearly in the time domain in figure 5.1. When adding the final case, targeting a final SoC of 90 %, the solution differs from the shape of the previous cases, as seen in figure 5.2. This can be explained by the activation of the upper battery constrained, described in section 3.3.1, which prevents the overcharging of the power storage system and therefore changes the shape of the solution.

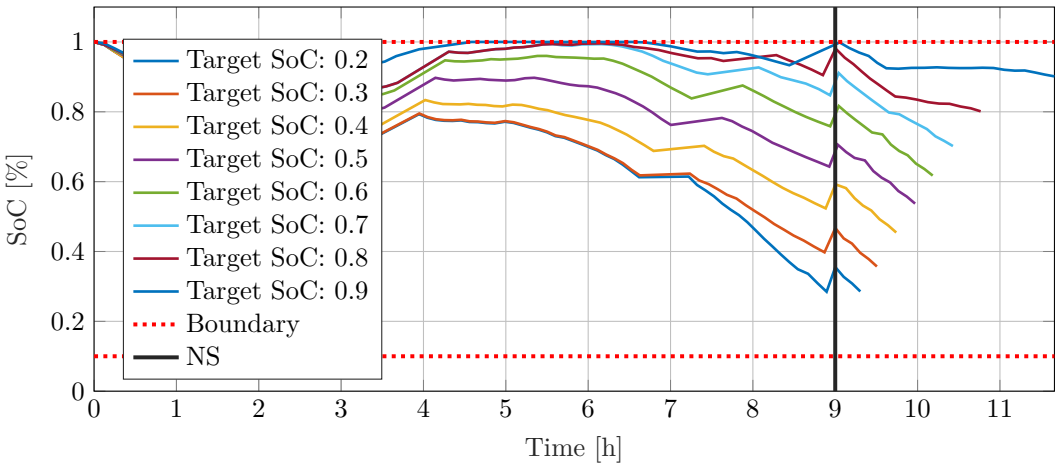

Figure 5.2: Battery sweep in time domain (target SoC between 0.2 % and 0.9 %)

5.1.2 Validation Through Correlation

The correlation between the targeted SoC and the final time, average velocity, and average input show the expected linear relationship as seen in figures 5.3, 5.4, and 5.5. It can clearly be seen that a lower targeted SoC leads to a higher average input, a higher average velocity, and a lower final time. The outlier originating from the 90 % case can clearly be seen and is marked in red.

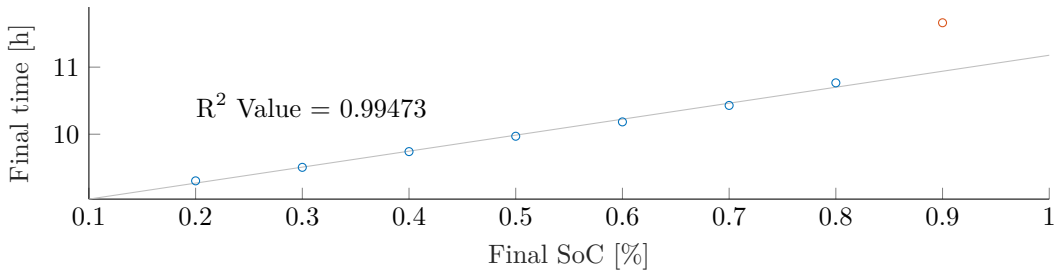

Figure 5.3: Correlation between final *SoC* and final time for battery sweep

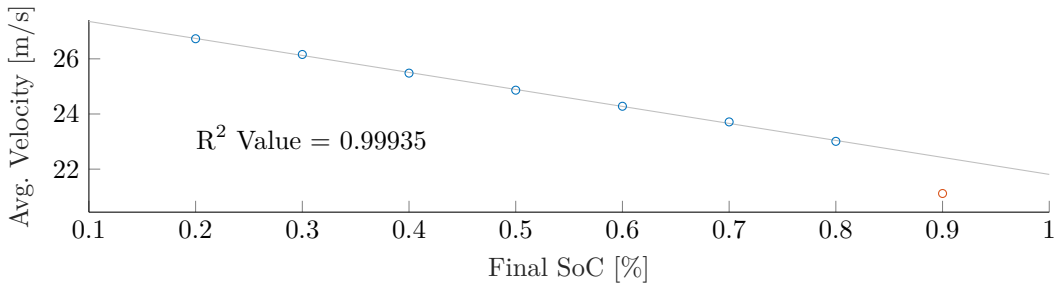

Figure 5.4: Correlation between final *SoC* and average velocity for battery sweep

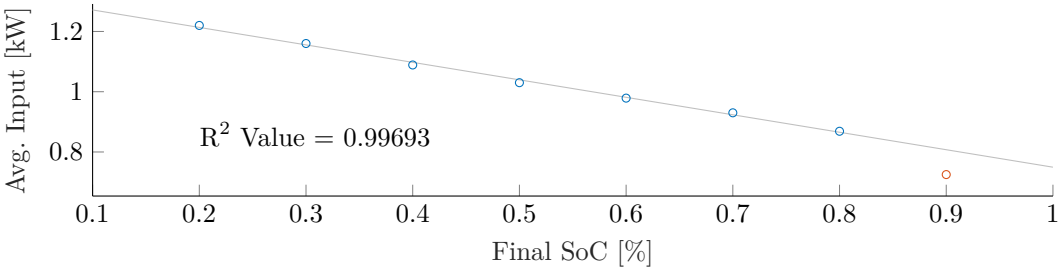

Figure 5.5: Correlation between final *SoC* and average input for battery sweep

5.2 Case Study 2: Solar Parameter Sweep

In the second case study, the varying parameter scales the global irradiance acting onto the system, as shown in figure 5.6. The objective is to see how the system reacts when it is starved of energy. The optimization for each iteration was over a distance of 800 km and took a computational time of 10 min.

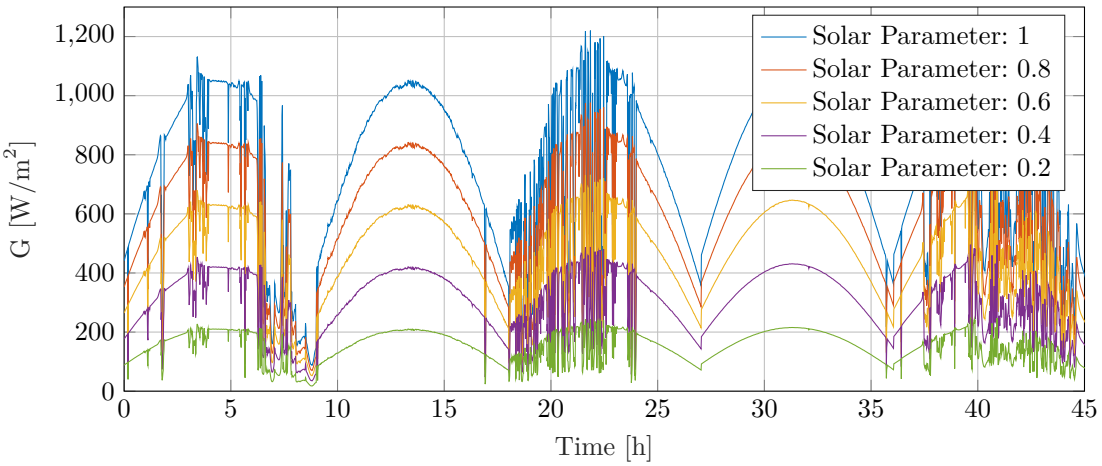

Figure 5.6: Global irradiance scaled with solar sweep parameter

5.2.1 Results

The results of this case study can be split into two parts: an energy non-constrained and an energy constraint part.
The cases classifiable as energy non-constrained are shown in 5.7. Here, the system can compensate for the lower amount of energy available, by decreasing the final *SoC*. For both cases presented, the final time, velocity profile, and input profile are identical.

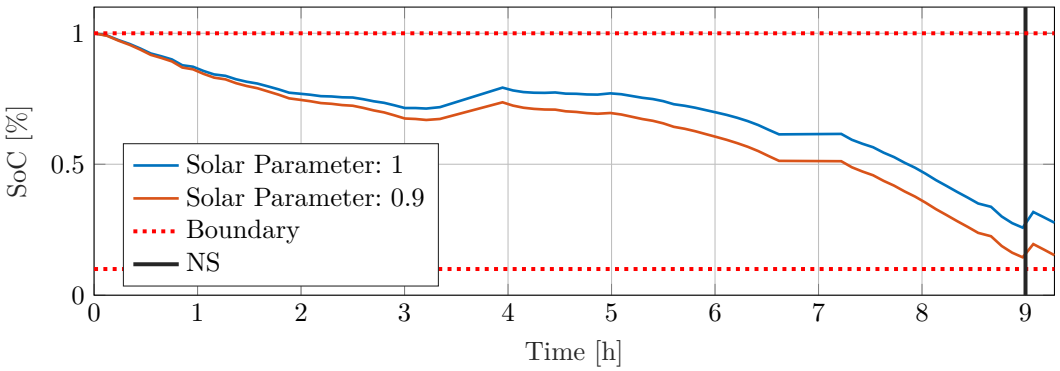

Figure 5.7: Solar parameter sweep between 0.9 and 1 in time domain

When adding the next result of the sweep, as seen in figure 5.8, the lower amount of energy available cannot be compensated by lowering the final *SoC* value anymore, since the 10 % battery constraint, as described in section 3.3.1, would be violated. Therefore, the final time needs to be increased to still make it to the targeted final distance.

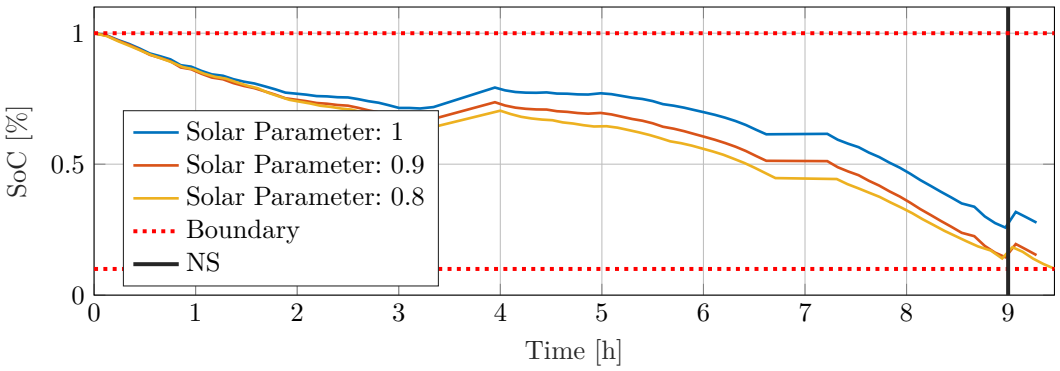

Figure 5.8: Solar parameter sweep between 0.8 and 1 in time domain

This trend continues for all following results, as seen in figure 5.9.

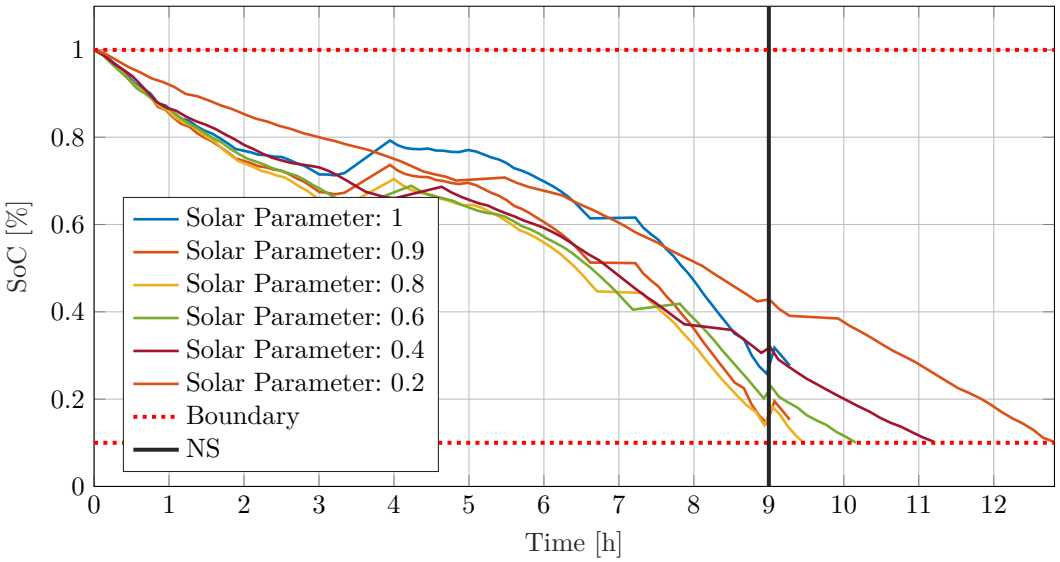

Figure 5.9: Solar parameter sweep between 0.2 and 1 in time domain

5.2.2 Validation Through Correlation

The correlation between the solar sweep parameter and the final time, average velocity, and average input show the expected linear relationship as seen in figures 5.10, 5.11, and 5.12. One can clearly see that a higher solar parameter leads to a higher average input and velocity, which lowers the final time.
The outlier originating from the 1 and 0.9 cases can clearly be seen and are marked in red. Once the solar parameter becomes larger than 0.8 the system won't be energy-constrained anymore and will always choose the solution with the maximal velocity profile conforming with the boundaries defined in section 3.3.1. For this reason, the average input, average velocity, and final time will be identical.

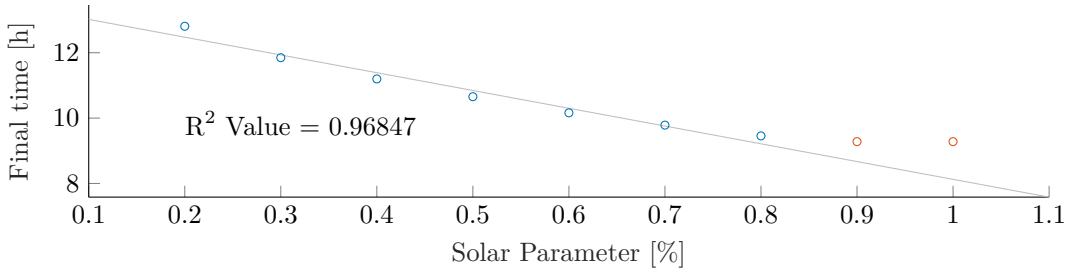

Figure 5.10: Correlation between solar parameter and final time

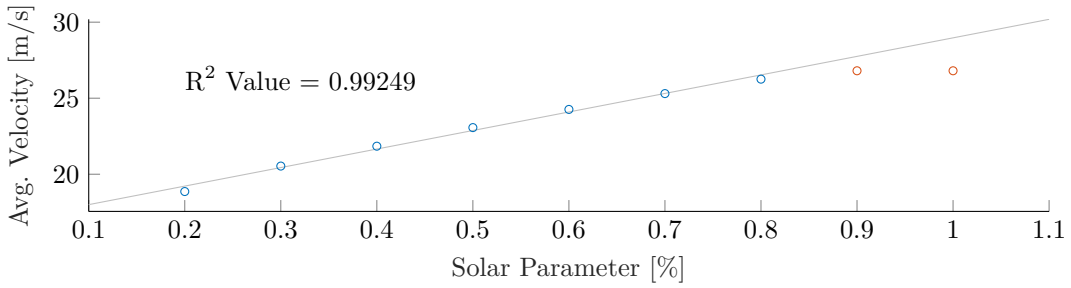

Figure 5.11: Correlation between solar parameter and average velocity

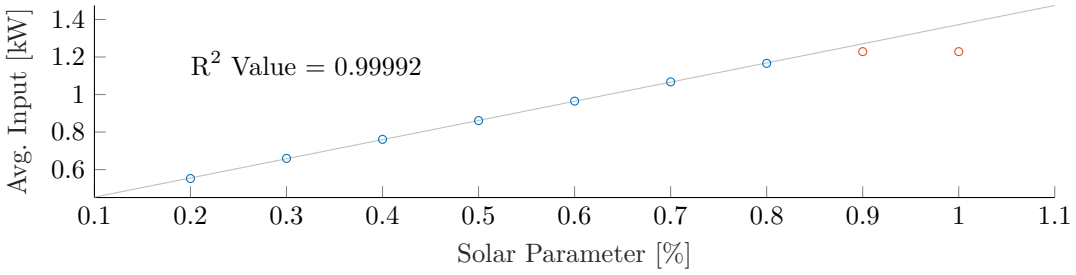

Figure 5.12: Correlation between solar parameter and average input

5.3 Case Study 3: Solar "Wall" Sweep

In the third and final case study, the global irradiance is modeled as a step function from 0 $^{W}/_{m^2}$ to 1200 $^{W}/_{m^2}$, where the sweep parameter is correlated to the distance from the start of the race to the activation of the step, as seen in figure 5.13.
The objective of this case study is to starve the system of energy until a certain point in time is reached, after which it will be abundant, and to assess its behavior.
The optimization for each iteration was over a distance of 800 km and took a computational time of 10 min.

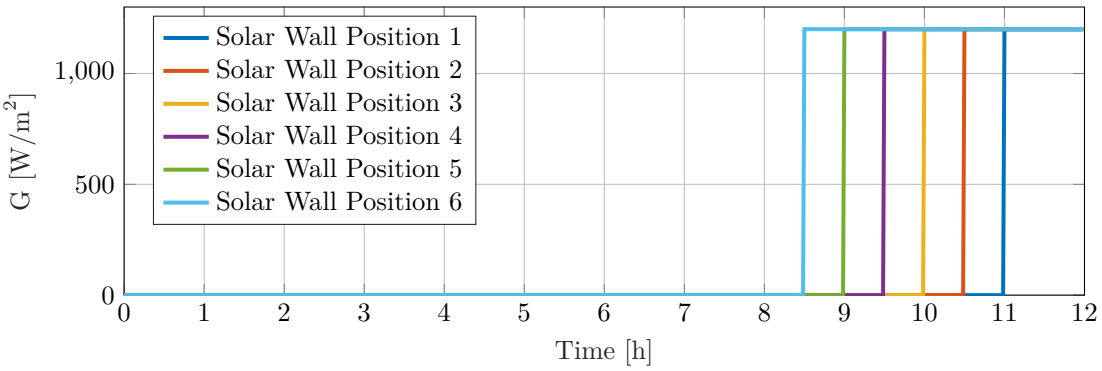

Figure 5.13: Case study 3 global irradiance modeled with step function (sweep 1-6)

5.3.1 Results

Selected sweeps of this case study can be seen in figures 5.14 and 5.15 in the time and space domain respectively.
In the space domain, all cases end up with a final SoC value of 10 %, while one can clearly see a deviation in the final time in the time domain. Like in case study 2, the system is energy constrained and needs to adapt the final time state in order to reach the final destination when the energy input is changed. One can also clearly notice the shifting of the control stops in the time domain. Less energy available means lower average velocities and therefore the stops will be reached at a later time.

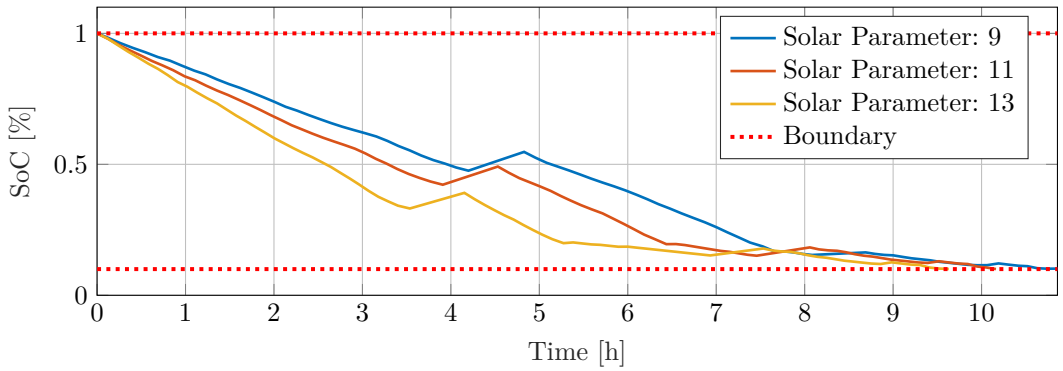

Figure 5.14: Solar wall sweep with parameters 9, 11, and 13 in time domain

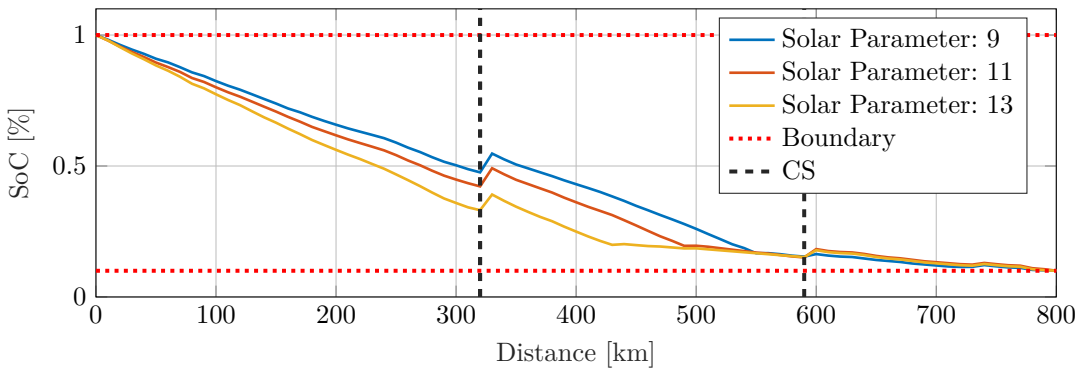

Figure 5.15: Solar wall sweep with parameters 9, 11, and 13 in space domain

5.3.2 Validation Through Correlation

The correlation between the solar wall parameter and the final time, average velocity, and average input show the expected linear relationship as seen in figures 5.16, 5.17, and 5.18. More energy means a higher average input and velocity, which in turn leads to a lower final race time.
One can see a slight change in the linear correlation around wall parameter 7. This is the point where the solar step crosses the second control stop. This changes the optimization behavior in a non-linear way, which shows in the correlation graphs.

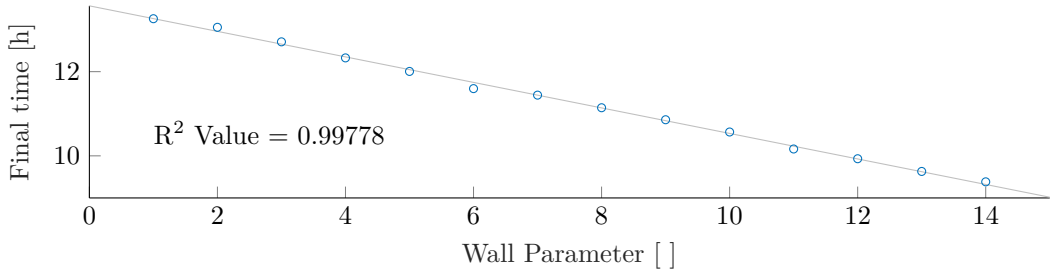

Figure 5.16: Correlation between solar wall parameter and final time

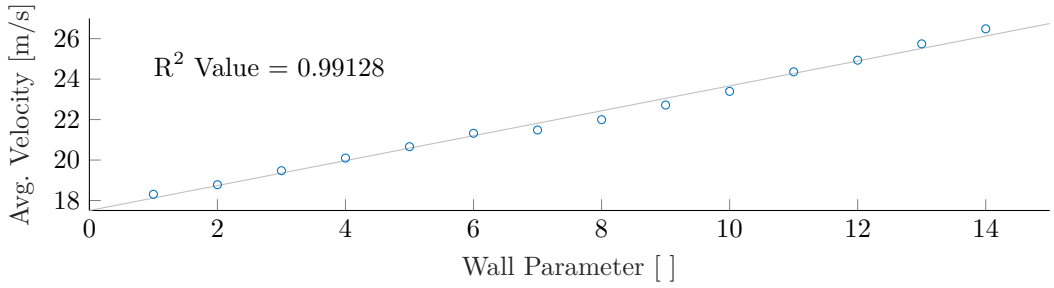

Figure 5.17: Correlation between solar wall parameter and average velocity

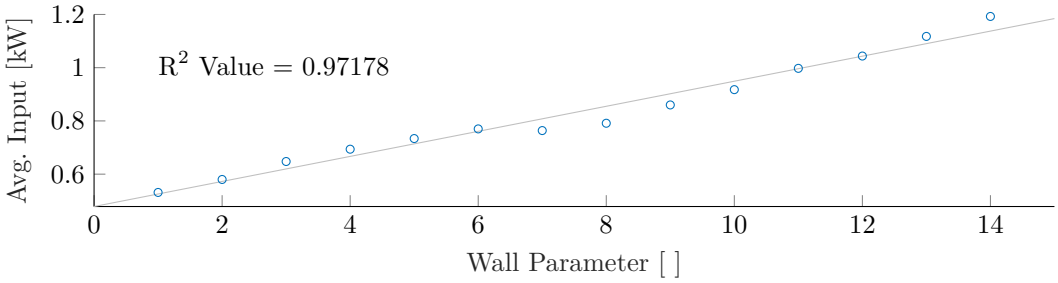

Figure 5.18: Correlation between solar wall parameter and average input

Chapter 6

Conclusion and Outlook

In this chapter, the final conclusion of the work conducted during this Semester Project and an Outlook will be given. The outlook focuses on identifying future work packages to improve the found strategy for the *aCentauri Solar Racing Team* and the *Bridgestone World Solar Challenge*.

6.1 Conclusion

In conclusion, all relevant dynamics of the solar-powered car were modeled and the defined system shows all expected behaviors correctly. Furthermore, the dynamic programming approach was successfully used in order to find an optimal long-term race strategy for the *Bridgestone World Solar Challenge*.
Moreover, the created algorithm proved to be very versatile and can be easily adapted to facilitate future races, competitions, and car designs. This provides the *aCentauri Solar Racing Team* with a powerful tool to efficiently find an optimized race strategy in all project cycles to come.
Furthermore, the optimization algorithm was validated through correlation with the help of different case studies, where the expected behavior could be observed.

6.2 Outlook

Like in most engineering projects, there are always ways to continue to improve and build upon a solution and this Semester Thesis is no exception to this rule. In order to get to the ideal point with regard to the race strategy for the BWSC, the following tasks are still outstanding:

- Improving the system models: This includes the models mentioned in section 2.5 for the temperature of the PV system. Furthermore, more losses on the mechanical and electrical side of the solar-powered car will be investigated and implemented.
- Adding space dependency for global irradiance. This input is currently only time-dependent, due to the lack of accurate data, as mentioned in section 2.6.
- Implementing an online short-term strategy with higher spatial resolution in the range of 1 km and frequent strategy updates for the driver based on an MPC approach.
- Many other teams struggled with their cars flipping over, due to the strong winds encountered at the end of the route near Adelaide. Therefore, the tilting behavior of the car will be researched, modeled, and implemented in the optimization as a constraint.
- Lastly, after the competition is completed in late October 2023, the entire system model, optimization, and race strategy will be analyzed with the measured real-world data.

Bibliography

[1] ETH Zürich, "Fokus-Projekte," https://ethz.ch/, 2023, [Online; Accessed: 2023-06-20].

[2] Tribecraft AG, *Renderings of aCentauri Solar Race Car.* Tribecraft, 2023.

[3] ETH Zürich, "aCentauri Solar Racing Team," https://www.acentauri.ch/, 2023, [Online; Accessed: 2023-05-15].

[4] Bridgestone World Solar Challenge, https://worldsolarchallenge.org/, 2023, [Online; Accessed: 2023-06-22].

[5] ——, "2023 Event Regulations," https://worldsolarchallenge.org/files/2268_2023_bwsc_regulations_release_version_2_published_24_02_2023_final.pdf, 2023, [Online; Accessed: 2023-06-25].

[6] L. Guzzella and A. Sciarretta, *Vehicle Propulsion Systems: Introduction to Modeling and Optimization.* Springer, 01 2007.

[7] M. Daniel and P. Kumar, "Racing with the sun: the optimal use of the solar power automobile," in *Proceedings of the 36th IEEE Conference on Decision and Control*, vol. 1, 1997, pp. 571–576 vol.1.

[8] Prof. Dr. Raffaello D'Andrea, "Lecture notes: Dynamic programming and optimal control," ETH Zürich, Fall 2022.

[9] O. Sundstrom and L. Guzzella, "A generic dynamic programming matlab function," in *2009 IEEE Control Applications, (CCA) Intelligent Control, (ISIC)*, 2009, pp. 1625–1630.

[10] Institute for Dynamic Systems and Control, "Proprietary dynamic programming software," June 2023.

[11] Dr. Stijn van Dooren, Personal Communication, April 2023, IDSC.

[12] aCentauri Solar Racing Team, Personal Communication, June 2023.

[13] G. Copper, "Lecture notes: Photovoltaic system modeling and analysis," School of Photovoltaics and Renewable Energy Engineering, UNSW Sydney, Australia, 2018.

[14] J. J. Roberts, A. A. Mendiburu Zevallos, and A. M. Cassula, "Assessment of photovoltaic performance models for system simulation," *Renewable and Sustainable Energy Reviews*, vol. 72, pp. 1104–1123, 2017. [Online]. Available: https://www.sciencedirect.com/science/article/pii/S1364032116306712

[15] R. J. Ross and M. Smokler, "Flat-plate solar array project final report," pp. 86–31, 1986.

[16] Australian government, bureau of meterology, http://www.bom.gov.au/climate/data/oneminsolar/about-IDCJAC0022.shtml, 2022, [Online; Accessed: 2022-09].

[17] Institute for atmospheric and climate science, https://iac.ethz.ch/, 2022, [Online; Accessed: 2022-12].

[18] Brouter, "," https://brouter.de/brouter-web/#map=5/50.990/9.860/standard, 2022, [Online; Accessed: 2022-12].

ETH zürich

Institute for Dynamic Systems and Control

Prof. Dr. R. D'Andrea, Prof. Dr. E. Frazzoli, Prof. Dr. Lino Guzzella, Prof. Dr. C. Onder, Prof. Dr. M. Zeilinger

Title of work:

Strategy Optimization for the Bridgestone World Solar Challenge Using Dynamic Programming

Thesis type and date:

Semester Project, June 2023

Supervision:

Giona Fieni
Marc-Philippe Neumann
Prof. Dr. Christopher Onder

Student:

Name: Severin Meyer
E-mail: sevmeyer@student.ethz.ch
Legi-Nr.: 18-926-857
Semester: FS 2023

Statement regarding plagiarism:

By signing this statement, I affirm that I have read and signed the Declaration of Originality, independently produced this paper, and adhered to the general practice of source citation in this subject-area.

Declaration of Originality:

`https://www.ethz.ch/content/dam/ethz/main/education/rechtliches-abschluesse/leistungskontrollen/declaration-originality.pdf`

Zurich, 25.6.2023: _____